Far-infrared Reflection Spectra, Optical and Dielectric Constants, and Lattice Vibrations of Some Fluoride Crystals

Ichiro NAKAGAWA

Department of Chemistry, Faculty of Science, The University of Tokyo, Hongo, Tokyo

(Received June 11, 1971)

The reflection spectra of the crystals of the NaCl structure (LiF, NaF, and NiO), the fluorite structure (CaF_2, BaF_2, and CdF_2), and the rutile structure (MgF_2 and MnF_2) were measured. The optical and dielectric constants were derived from the measured reflectivities using the Kramers-Kronig transformation. The absorption indices (k) for these crystals are rather large and the peak values of the imaginary dielectric constants amount to 30.0 or more. However, unlike the ferroelectric substances such as oxide perovskites and rutile, these fluoride crystals do not show any anomalous dielectric behaviour. From the real and imaginary dielectric constants $\varepsilon'(\nu)$ and $\varepsilon''(\nu)$, the transverse and longitudinal frequencies for the lattice modes are determined. These frequencies are reasonably interpreted on the basis of the crystal structures and satisfy the Lyddane-Sachs-Teller relation. The effective charge on the positive and negative ions and the force constant associated with the short-range elastic force against the ion displacement are obtained for the cubic crystals.

Several investigations on the optical and dielectric properties of the fluoride crystals have been made using reflection data as well as transmission spectra by Hunt and Perry,[1] Perry,[2] Barker,[3] Axe and Pettit,[4] Balkanski *et al.*,[5] Bosomworth,[6] and Denham *et al.*[7] In the course of our studies on the lattice vibrations of inorganic salts, we have investigated the transmission spectra of some fluoride perovskites.[8,9] On the basis of the dynamical model we obtained the potential constants associated with the short-range repulsive force without taking into account the long-range interaction. The longitudinal frequencies as well as the transverse frequencies supply further information on the interionic forces in the crystal, specifically on the long-range, electrostatic interaction.

The purpose of the present study is to establish the optical and dielectric constants of various kinds of fluoride crystals from the reflectivity data and to determine the longitudinal frequencies as well as the transverse frequencies for the crystal lattice modes, by which the effective charge on the positive and negative ions can be obtained.

The crystals investigated are those of the NaCl structure (LiF, NaF, and NiO), the fluorite structure (CaF_2, BaF_2, and CdF_2), and the rutile structure (MgF_2 and MnF_2). Reflection and transmission measurements for crystals other than MnF_2 and NiO have been made by several researchers. Except for the fluorites, however, the data are rather old and the observed frequency range and procedure for obtaining the frequencies are not always satisfactory. It is therefore worth while to make a remeasurement for these crystals also and compare the optical and dielectric constants and the lattice frequencies determined in different laboratories with one another, since the procedure for obtaining these parameters is not straightforward and contains a wide variety of technique.

Experimental

The room temperature reflectivity at near normal incidence was measured down to 30 cm^{-1} with a Hitachi FIS-21 single-beam vacuum far infrared spectrometer attached with a specular reflectance accessary (incidence angle 11°). The reflectivity measurement in the region 700—300 cm^{-1} was made with a Hitachi EPI-L double-beam infrared spectrometer attached with a IRR-3 type reflectance accessary (incidence angle 12°).

For the measurement of a crystal of small dimension (~5 mm × 5 mm), a reflectance attachment with two spherical mirrors and two plane mirrors was designed for the use of a Hitachi FIS-1 vacuum infrared spectrometer as a single-beam use, as shown in Fig. 1 (incidence angle 10°).

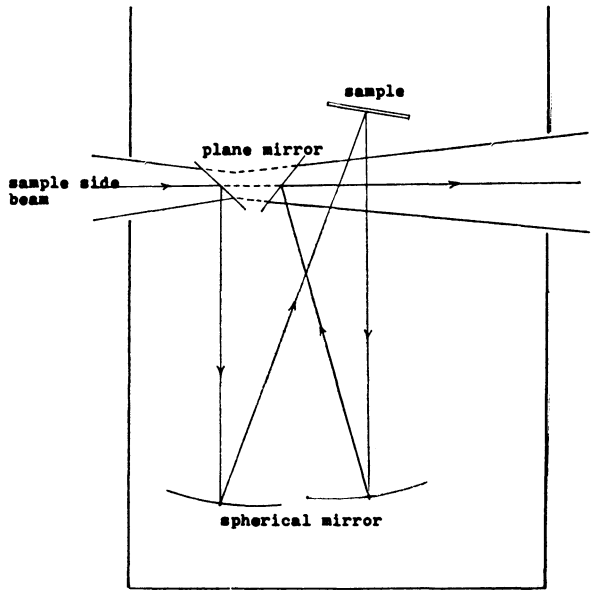

Fig. 1. Specular Reflectance Accessary for a Crystal of Small Dimension Attached to a Hitachi FIS-1 Spectrometer.

1) G. R. Hunt and C. H. Perry, *Phys. Rev.*, **134**, A188 (1964).
2) C. H. Perry, *Japanese J. Appl. Phys.*, **4, Suppl. I**, 565 (1965).
3) A. S. Barker, *Phy. Rev.*, **136**, A1290 (1964).
4) J. D. Axe and G. D. Pettit, *Phys. Rev.*, **157**, A435 (1967).
5) M. Balkanski, P. Moch, and G. Parisot, *J. Chem. Phys.*, 44, 940 (1966).
6) D. P. Bosomworth, *Phys. Rev.*, **157**, A709 (1967).
7) P. Denham, G. R. Field, P. L. R. Morse, and G. R. Wilkinson, *Proc. Roy. Soc. London, Ser. A*, **317**, 55 (1970).
8) I. Nakagawa, A. Tsuchida, and Shimanouchi, *J. Chem. Phys.*, **47**, 982 (1967).
9) K. Kohn and I. Nakagawa, This Bulletin **43**, 3780 (1970).

Determination of Optical Constants

The optical and dielectric constants, n(refractive index), k(absorption index), ε' and ε''(real and imaginary dielectric constants), are derived from the measured reflectivity using the Kramers-Kronig relation.[10] At normal incidence it is possible to proceed from a measurement of R(the reflectivity for unpolarized radiation), since the distinction between R_s and R_p (the reflectivities for perpendicular and parallel polarized radiations) is meaningless. The complex reflected amplitude ($\hat{r}$) is expressed in terms of its phase angle θ as

$$\hat{r} = |r| \exp(i\theta) = \sqrt{R} \exp(i\theta) = \frac{n-ik-1}{n-ik+1}, \tag{1}$$

from which one obtains

$$n = \frac{1-R}{1+R-2\sqrt{R}\cos\theta}, \tag{2}$$

$$k = \frac{-2\sqrt{R}\sin\theta}{1+R-2\sqrt{R}\cos\theta}, \tag{3}$$

$$\varepsilon' = n^2 - k^2, \tag{4}$$

$$\varepsilon'' = 2nk. \tag{5}$$

The phase angle θ at any particular frequency ν_0 is calculated by the Kramers-Kronig transformation

$$\theta(\nu_0) = \frac{2\nu_0}{\pi}\int_0^\infty \frac{\ln R(\nu)}{\nu^2-\nu_0^2}\,d\nu. \tag{6}$$

The reflectivity measurements are limited to some finite spectral region(ν_L to ν_H), and the correction terms due to the contributions from all the frequencies above the high-frequency limit(ν_H) and below the low-frequency limit(ν_L) were calculated according to the procedure proposed by Roessler.[11] The value of $\theta(\nu_0)$ is given as

$$\theta(\nu_0) = \frac{2\nu_0}{\pi}\int_{\nu_L}^{\nu_H} \frac{\ln R(\nu) - \ln R(\nu_0)}{\nu^2-\nu_0^2}\,d\nu + \frac{1}{2\pi}\ln\left|\frac{\nu_0-\nu_L}{\nu_0+\nu_L}\right| \ln\left[\frac{R(\nu_L)}{R(\nu_0)}\right] - \frac{1}{2\pi}\ln\left|\frac{\nu_H-\nu_0}{\nu_H+\nu_0}\right| \ln\left[\frac{R(\nu_H)}{R(\nu_0)}\right]. \tag{7}$$

Numerical integration of Eq. (7) and subsequent calculations of the optical and dielectric constants were performed with a HITAC 5020E Computer of the Computation Center, the University of Tokyo. The measured reflectivity data and the obtained optical and dielectric constants are shown in Figs. 2~9.

Transverse and Longitudinal Optical Frequencies

On the basis of the damped oscillator model with several modes, the dielectric constants are expressed as

$$\varepsilon'(\nu) = \varepsilon_\infty + \sum_j 4\pi\rho_j\nu_j^2 \frac{\nu_j^2-\nu^2}{(\nu_j^2-\nu^2)^2+\gamma_j^2\nu^2}, \tag{8}$$

$$\varepsilon''(\nu) = \sum_j 4\pi\rho_j\nu_j^2 \frac{\gamma_j\nu}{(\nu_j^2-\nu^2)^2+\gamma_j^2\nu^2}, \tag{9}$$

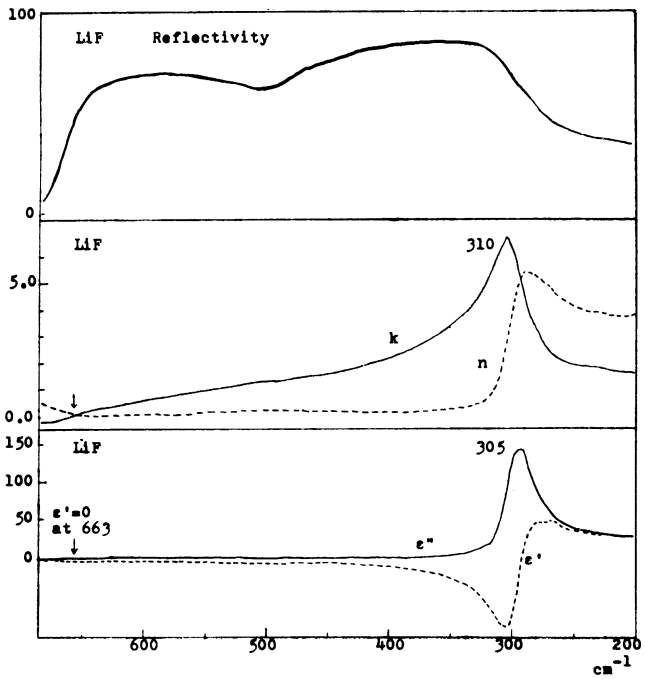

Fig. 2. Reflectivity, Optical Constants (n and k), and Dielectric Constants (ε' and ε'') of LiF.

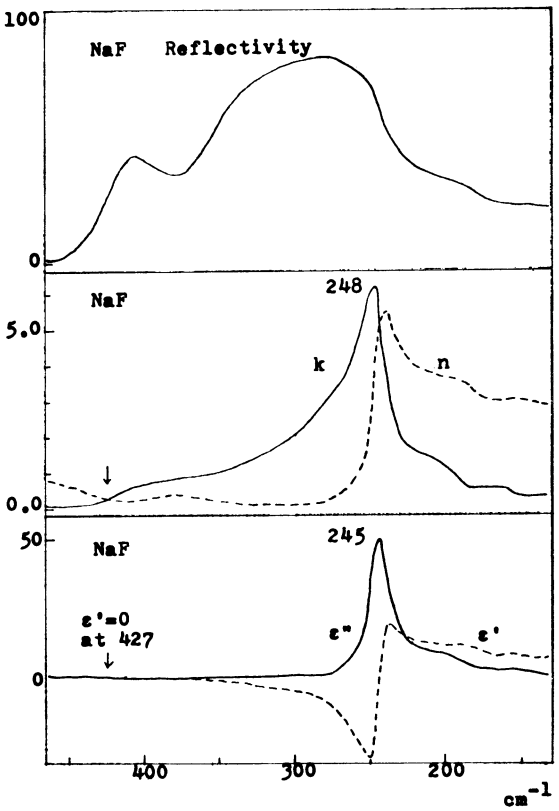

Fig. 3. Reflectivity, Optical Constants (n and k), and Dielectric Constants (ε' and ε'') of NaF.

10) T. S. Robinson and W. C. Price, *Proc. Phys. Soc., Ser. B*, **66**, 969 (1953).

11) D. M. Roesller, *Brit. J. Appl. Phys.*, **16**, 1119 (1965); **17**, 1313 (1966).

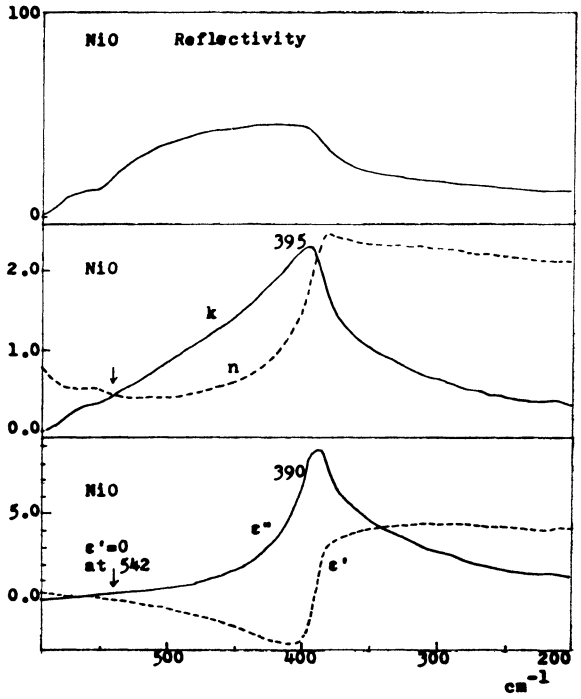

Fig. 4. Reflectivity, Optical Constants (n and k), and Dielectric Constants (ε' and ε'') of NiO.

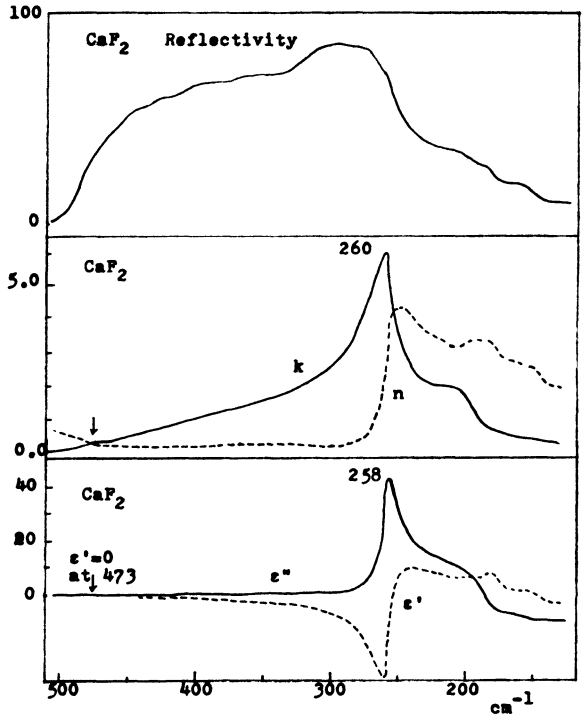

Fig. 5. Reflectivity, Optical Constants (n and k), and Dielectric Constants (ε' and ε'') of CaF_2.

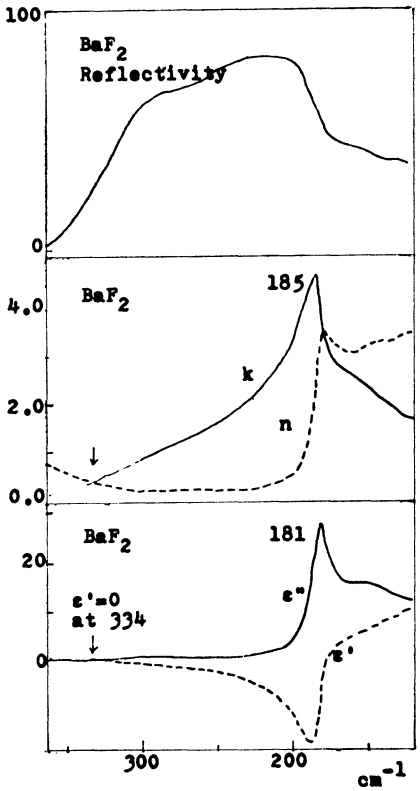

Fig. 6. Reflectivity, Optical Constants (n and k), and Dielectric Constants (ε' and ε'') of BaF_2.

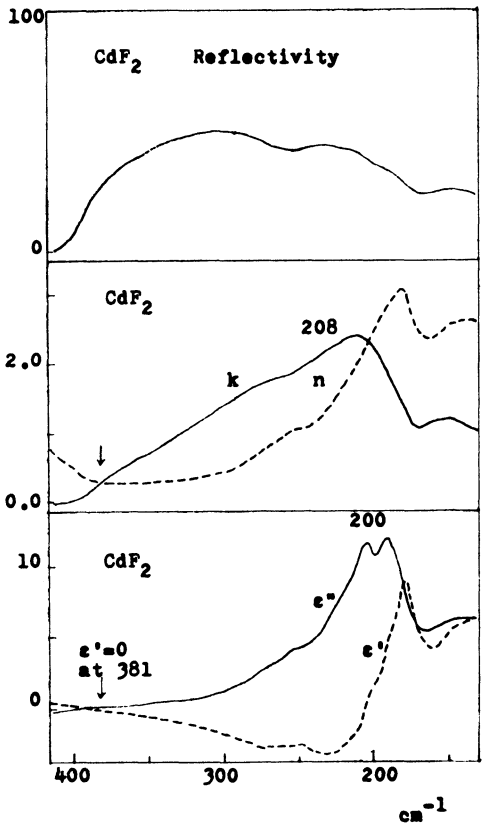

Fig. 7. Reflectivity, Optical Constants (n and k), and Dielectric Constants (ε' and ε'') of CdF_2.

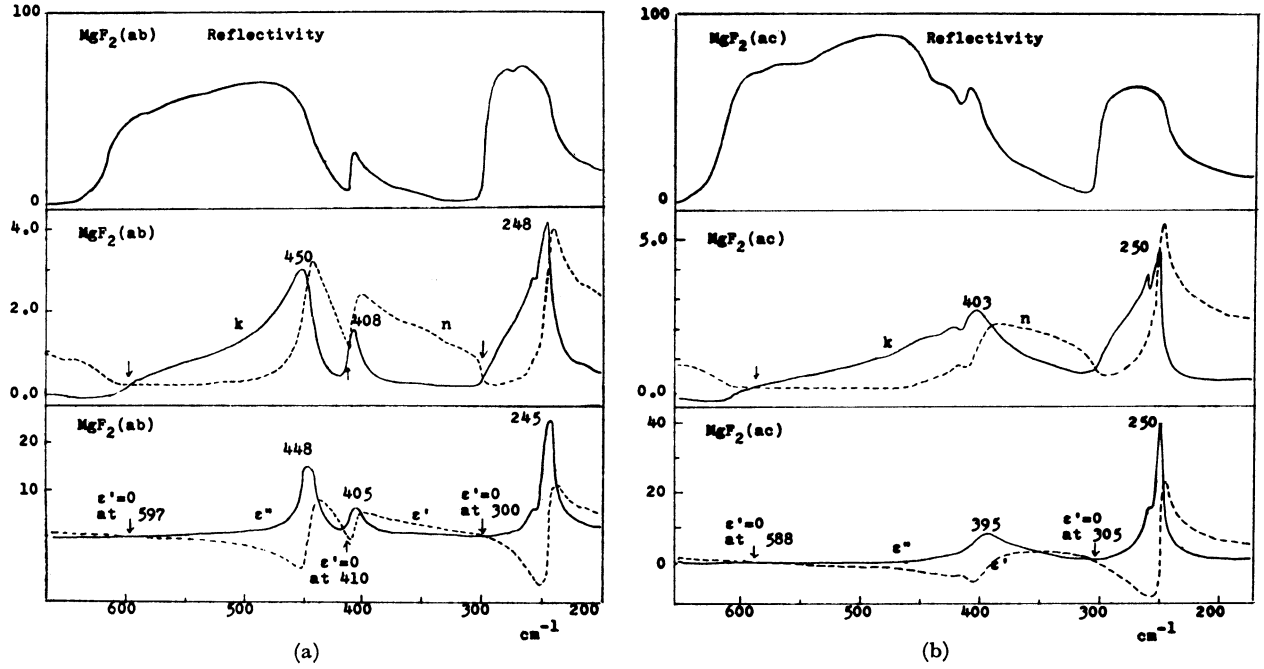

Fig. 8. Reflectivity, Optical Constants (n and k), and Dielectric Constants (ε' and ε'') of MgF_2. (a) Reflection of ab-plane (b) Reflection of ac-plane.

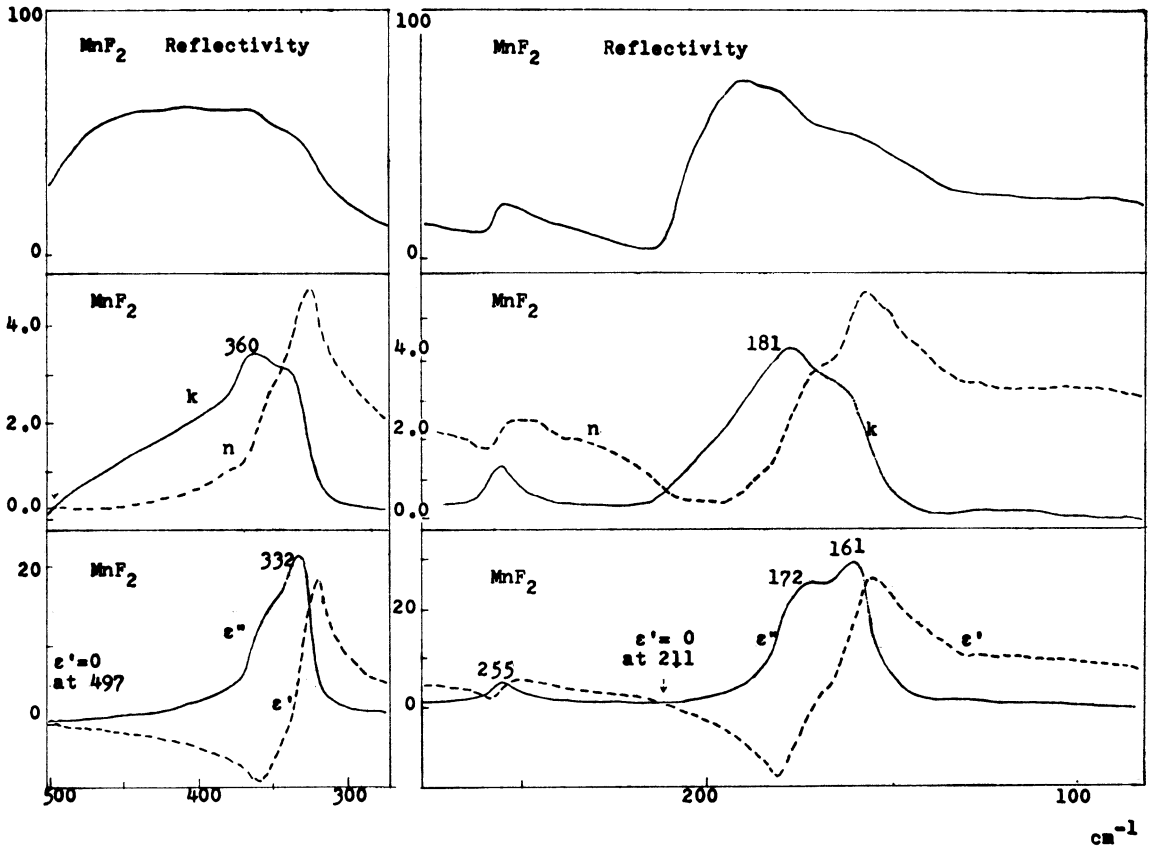

Fig. 9. Reflectivity, Optical Constants (n and k), and Dielectric Constants (ε' and ε'') of MnF_2.

where ν_j, ρ_j and γ_j are the resonance frequency, oscillator strength and damping constant, respectively, of the j-th mode. It is found from Eqs. (8) and (9) that for the small damping γ_j the poles of $\varepsilon'(\nu)$ curve and the maxima of $\varepsilon''(\nu)$ curve coincide and they are located around $\nu=\nu_j$. These frequencies give the optically active lattice frequencies of the long-wavelength transverse modes.[3,4] The corresponding longitudinal frequencies are given by the frequencies where $\varepsilon'(\nu)$ becomes zero in changing from negative to positive values.[3,4,12]

TABLE 1. SUMMARY OF TRANSVERSE AND LONGITUDINAL FREQUENCIES IN cm^{-1}

Crystals	ν_T	ν_{pole}	σ_{max}	ν_L	
LiF	305	305	305	663	
LiF	304			660	Ref. (13)
NaF	245	245	245	427	
NaF	246			424	Ref. (13)
NiO	390	392	390	542	
CaF_2	258	255	258	473	
CaF_2	266		266	474	Ref. (7)
CaF_2	257			463	Ref. (6)
BaF_2	181	180	181	334	
BaF_2	189		189	330	Ref. (7)
BaF_2	184			331	Ref. (6)
CdF_2	200	200	205	381	
CdF_2	209		209	404	Ref. (7)
CdF_2	202			380	Ref. (6)
MgF_2	448	446	448	597	
	405	(406)	405	410	
(*ab*-plane)	(258sh)				
	245	246	245	300	
MgF_2	395	390	395	588	
(*ac*-plane)	(260sh)				
	250	250	250	305	
MgF_2	435				
	405				
	280				Ref. (1)
	265				
$MgF_2(E\perp c)$	450			617	Ref. (3)
	410			415	
	247			303	
$MgF_2(E//c)$	399				
	not observed				Ref. (3)
MnF_2	(357sh)				
	332	340	332	497	
	255				
	172	172	173	211	
	161		161		

ν_T: transverse frequencies, ν_L: longitudinal frequencies, ν_{pole}: pole of $\varepsilon'(\nu)$ curve, σ_{max}: peak of conductivity, sh: shoulder.

The transverse and longitudinal frequencies determined by the procedure mentioned above are listed in Table 1. This table also includes the results of other researchers for some of the crystals, since a comparison of the frequencies from different sources is significant to justify various methods for the determination of the transverse and longitudinal frequencies. The argument for each type of crystal listed in Table 1 will be given in the following.

Crystals of NaCl structure. For this type of crystal one infrared active mode is observed as a transverse component and a longitudinal component. The peak values of absorption index(k) and imaginary dielectric constant(ε'') are very large for LiF and NaF, while those for NiO are rather small.

Crystals of fluorite structure. The crystal of this type has the space group O_h^5 with one formula unit and one f_{1u} mode is infrared active. The transverse frequencies of CaF_2, BaF_2 and CdF_2 obtained by this study are in agreement with those by Denham *et al.*[7] and by Bosomworth.[6] The longitudinal frequency of CdF_2 by Denham *et al.* which was determined using the Berreman method[14] by depositing a thin film on a mirror surface differs slightly from that by the present study and by Bosomworth.

Crystals of rutile structure. MgF_2 and MnF_2 have this structure with the space group D_{4h}^{14} and the Bravais primitive cell contains two formula units. This type of crystal is not cubic but uniaxial and 1 $a_{2u}(E//c\text{-axis})$ and 3 $e_u(E\perp c\text{-axis})$ lattice modes are infrared active. As is shown in Fig. 8 the reflectivities of the *ab*-plane and *ac*-plane for MgF_2 are somewhat different. The transverse and longitudinal frequencies obtained in both cases also differ to some extent as is seen in Table 1. From the result of the *ab*-plane measurement shown in Fig. 8(a), the e_u mode frequencies are determined as 448 cm^{-1}, 405 cm^{-1}, and 245 cm^{-1}, which are in good agreement with those obtained by Barker using a $E\perp c$ polarized radiation.[3] In the *ac*-plane measurement, if the crystal is set properly so that the *c*-axis may take a direction perpendicular to the incidence plane, the two peaks of $k(\nu)$ and $\varepsilon''(\nu)$ around 400 cm^{-1} observed in the *ab*-plane spectrum do not appear clearly and instead one peak at 395 cm^{-1} is observed as shown in Fig. 8(b). This *ac*-plane spectrum of Fig. 8(b) is similar to that of $E//c$ by Barker, superimposed with a small amount of *ab*-plane spectrum, though Barker only carried out measurement down to 280 cm^{-1} and could not observe the peak around 250 cm^{-1}. From the above result it is concluded that the peak at 395 cm^{-1} is related to the a_{2u} species and the one around 250 cm^{-1} may also arise from the a_{2u} mode.

For MnF_2 crystal, a sample having sufficient area for the *ab*-plane and *ac*-plane could not be obtained, and accordingly the symmetry species of the observed transverse frequencies have not been determined experimentally. However, the plane for which the reflectivity measurement was performed was found to be almost 101 plane by crystal analysis. Due to the closeness of the transverse frequencies of 172 cm^{-1} and 161 cm^{-1}, two corresponding longitudinal frequencies could not be determined.

Discussion

The dielectric constants $\varepsilon'(\nu)$ and $\varepsilon''(\nu)$ were well interpreted on the basis of the lattice modes expected from the crystal symmetry, except for very weak extra

12) M. Born and K. Huang, "*Dynamical Theory of Crystal Lattices*," (*Oxford University Press, New York, 1954*).

13) D. H. Martin, *Advan. Phys.*, **14**, 39 (1965).

14) D. W. Berreman, *Phys. Rev.*, **130**, 2193 (1963).

bands or shoulders contributed from another extra oscillators which may arise from (a) a forbidden transition, (b) a two-phonon process, or (c) a localized mode due to impurities or a crystal surface. The observed data of ν_T and ν_L frequencies are checked by the Lyddane-Sachs-Teller relation,[15]

$$\prod_j \frac{(\nu_L)_j}{(\nu_T)_j} = \left[\frac{\varepsilon_0}{\varepsilon_\infty}\right]^{1/2} \tag{10}$$

where ε_0 is a static dielectric constant and ε_∞ is a high-frequency dielectric constant and can be obtained from the refractive index for the visible light, n^2. In Table 2 the values of $\prod_j[(\nu_L)_j/(\nu_T)_j]$ calculated from the ν_T and ν_L frequencies determined in Table 1 are compared with $(\varepsilon_0/\varepsilon_\infty)^{1/2}$. The agreement is satisfactory.

Table 2. Application of Lyddane-Sachs-Teller relation to some fluoride crystals

	$\prod_j(\nu_L/\nu_T)_j$	$(\varepsilon_0/\varepsilon_\infty)^{1/2}$
LiF	2.17	2.20
NaF	1.74	1.86
CaF_2	1.83	1.81
BaF_2	1.84	1.82
CdF_2	1.90	1.88
MgF_2	1.65	1.68
(e_u)		

A short comment will be made concerning the peak values of $k(\nu)$ and $\varepsilon''(\nu)$. As described before there is some approximation in the procedure to get $k(\nu)$ and $\varepsilon''(\nu)$ curves, due to the limited range of the observed reflectivity data. According to the procedure utilized, the peak values of $k(\nu)$ and $\varepsilon''(\nu)$ are more or less affected but not those of ν_T and ν_L. Thus, no quantitative discussion on the peak values of $k(\nu)$ and $\varepsilon''(\nu)$ will be given. Nevertheless, it should be noted that for these ionic crystals of fluorides the values of the absorption indices(k) are rather large compared with those for liquid samples such as $CHCl_3$ and C_6H_6 (organic compounds)[16,17] and may take values larger than 2.0. ε'' may amount to 30.0 or more for the strong peaks, which are also much larger than the value of the order of 5.0 for liquid samples of organic compounds. However, it should be emphasized that the fluoride crystals studied here do not reveal any anomalous dielectric behavior, as compared with the dielectric constants of the oxide perovskites and rutile which amount to the order of 500.

Splitting of Transverse and Longitudinal Frequencies and Effective Charge

The transverse frequencies of some fluorides were analysed previously,[8,9] on the basis of the normal coordinate treatment of the dynamical model, taking into account the short-range interactions. Therefore, in the present treatment only the elastic force or restoring force against the ion displacement has been taken. The availability of the longitudinal frequencies as well as the transverse frequencies makes it possible to get information on factors other than the elastic force, such as electrostatic interaction.

On the basis of a polarizable ion model for the cubic diatomic crystals given by Born and Huang,[12] the transverse and longitudinal frequencies are derived as

$$4\pi^2\nu_T^2 = \frac{\beta}{\bar{M}} - \frac{4\pi}{3}\frac{1}{v}\left[\frac{Z^2e^2}{\bar{M}}\right]\left[1-\frac{4\pi}{3}\frac{\alpha^+ + \alpha^-}{v}\right]^{-1} \tag{11}$$

$$4\pi^2\nu_L^2 = \frac{\beta}{\bar{M}} + \frac{8\pi}{3}\frac{1}{v}\left[\frac{Z^2e^2}{\bar{M}}\right]\left[1+\frac{8\pi}{3}\frac{\alpha^+ + \alpha^-}{v}\right]^{-1} \tag{12}$$

where $\bar{M}$ is the reduced mass of unit cell ions$=M^+M^-/(M^+ + M^-)$, α^+ and α^- the ionic polarizabilities of the positive and negative ions, $\pm Ze$ the effective charge, β the force constant associated with the elastic force against the ion displacement, and $v=2(r_0/2)^3$ the volume of unit cell (r_0=cell constant). When the ions are assumed to be non-polarizable, this is reduced to a rigid ion model discussed by Denham *et al.*[7]

Eqs. (11) and (12) can be written in terms of ε_∞ instead of α^+ and α^- as

$$4\pi^2\nu_T^2 = \frac{\beta}{\bar{M}} - \frac{4\pi(Z^2e^2)(\varepsilon_\infty+2)}{9v\bar{M}}, \tag{13}$$

$$4\pi^2\nu_L^2 = \frac{\beta}{\bar{M}} + \frac{8\pi(Z^2e^2)(\varepsilon_\infty+2)}{9v\bar{M}\varepsilon_\infty}, \tag{14}$$

using Clausius Mosotti's relation

$$\frac{4\pi}{3}\frac{\alpha^+ + \alpha^-}{v} = \frac{\varepsilon_\infty - 1}{\varepsilon_\infty + 2}. \tag{15}$$

Eqs. (13) and (14) are reduced to the expressions based on a shell model developed by Cochran[18] and Axe.[19] Using the observed values of ν_T and ν_L listed in Table 1, the effective charges are obtained for both non-polarizable and polarizable ion models as shown in Table 3.

Table 3. Effective ionic charge (Z)

	I	II	III
LiF	0.77	0.81	0.82
NaF	0.80	0.85	0.93
NiO	0.81	a	a
CaF_2	0.80×2	0.85×2	0.83×2
BaF_2	0.84×2	0.90×2	0.88×2
CdF_2	0.77×2	0.82×2	0.80×2

I : Calculated based on a rigid ion model.
II : Calculated based on a shell model.
III: Calculated by Szigeti's formula.
a) The values of ε_∞ and ε_0 of NiO are not available.

Furthermore the following relation derived by Szigeti,[20] between ν_T and Ze expressed in terms of ε_0 and ε_∞

$$\nu_T^2 = \frac{1}{9\pi}\frac{(Z^2e^2)}{\bar{M}v}\frac{(\varepsilon_\infty+2)^2}{\varepsilon_0-\varepsilon_\infty}, \tag{16}$$

enables us to obtain Ze from the ν_T frequency for the crystals for which both ε_0 and ε_∞ are available. The

15) R. H. Lyddane, R. G. Sachs, and E. Teller, *Phys. Rev.*, **59**, 673 (1941).
16) T. Fujiyama and B. Crawford, Jr., *J. Phys. Chem.*, **72**, 2174 (1968).
17) B. Crawford, Jr., A. C. Gilby, A. A. Clifford, and T. Fujiyama, *Pure Appl. Chem.*, **18**, 373 (1969).
18) W. Cochran, *Advan. Phys.*, **9**, 387 (1960).
19) J. D. Axe, *Phys. Rev.*, **139**, A1215 (1965).
20) B. Szigeti, *Proc. Roy. Soc. London, Ser. A*, **204**, 51 (1950).

result is also given in Table 3.

In the infrared active mode of the XF_2 cubic crystal of fluorite structure, the reduced mass $\bar{M}=2M_FM_X/(2M_F+M_X)$ is used in Eqs. (11—16). $-Ze/2$, $-Ze/2$ and $+Ze$ correspond to the effective charges, respectively, on the two fluorine ions and on the metal ion.

In Table 3 it is found that the effective charge may be 15—20% below the formal charge for the fluoride crystals. However, for NiO the effective charge is 0.81 against the formal charge 2.0, which means that the electron delocalization is much larger in NiO than in the fluorides.

The contribution of factors other than the elastic force to the lattice frequencies can be estimated from the ratio of the second term of Eq. (11) to the first term for a rigid ion model. The ratio is given in Table 4 which also includes the short-range interionic elastic force constant $K(M\text{-}X)$. $K^*(M\text{-}X)$ is the calculated interionic force constant when the electrostatic term (second term) is neglected in Eqs. (11) and (13). It should be noted that the short-range elastic force constant between the positive and negative ions, calculated without taking into account the long-range electrostatic interaction, $K^*(M\text{-}X)$, is somewhat smaller than the true value $K(M\text{-}X)$.

TABLE 4. INTERIONIC RESTORING FORCE CONSTANTS IN mdyn/Å

	LiF	NaF	NiO	CaF_2	BaF_2	CdF_2
K(M-X)[a)]	0.31	0.31	0.74	0.51	0.39	0.47
K^*(M-X)	0.14	0.18	0.56	0.29	0.22	0.25
Ratio of Electrostatic term to Short-range Term	0.55	0.40	0.24	0.44	0.45	0.47

a) $K(M\text{-}X)=\frac{1}{2}\beta$ for MX crystals and $K(M\text{-}X)=(3/8)\beta$ for MX_2 crystals.

The author wishes to express his sincere thanks to Prof. Takehiko Shimanouchi, the University of Tokyo, for his encouragement and guidance. Thanks are also due to Prof. Akiyoshi Mitsuishi and Dr. Tetsuro Kawamura, Osaka University, for their kind instruction and suggestion on the Kramers-Kronig program and reflectivity measurement. A part of this work was supported by the RCA research grant.